C-band Continuum Source Spectra and Cold Sky Focus Offsets
Project TBASEJRF021230, December 30, 2002

Rick Fisher

January 20, 2003

Introduction

This is a standard set of baseline test observations on the C-band receiver to measure the response to a continuum source across the receiver frequency range, baseline changes caused by moving the subreflector in the Y direction, and stability of the continuum on-off spectra with time.

Setup

The C-band linearly polarized receiver channels X and Y were connected to fibers 2 and 3, respectively. The IF rack filters were set to either 2360 to 3640 or 2840 to 3160 MHz passband for 800 and 200 MHz spectrometer bandwidths, respectively. The analog filter rack outputs were set to 800 to 1600 or 800 to 1000 MHz passband. The spectrometer was set up for 800 bandwidth, 3-level, 2 samplers, 1 quadrant, 2048 channels per IF configuration (1W2-0XY-800) or 200 MHz bandwidth, 3-level, 2 samplers, 4 quadrants, 32768 channels per IF configuration (4W2-6XY-200). The signal path connections are shown in Table 1. An integration time of 30 seconds was used for all measurements. All 200-MHz spectra were smoothed by truncating the ACF at 2048 lags. All spectra were Hanning convolved.

The Measurements

Table 2 lists the telescope beam positions for the series of observations. Each line in this table corresponds to an on-off scan pair, where the 'off' position

Table 1: IF Rack to Spectrometer Connection Matrix

Rcvr	OR	CM	SF	Sampler
X	2	1	1	0
Y	3	5	5	1

Table 2: Telescope positions at the beginning of each scan or scan pair.

Source	Scans	UTC	Azimuth	Elevation	Frequency
NGC7027	3-4	22:21:15	-70.24	61.19	4300
NGC7027	6-7	22:33:47	-69.73	58.89	4700
NGC7027	8-9	22:45:41	-69.18	56.70	5100
NGC7027	10-11	22:57:23	-68.56	54.56	5500
HighElevEighth	13-14	23:27:34	256.6	66.89	5000
HighElevQuarter	15-16	23:38:17	259.3	64.83	5000
LowElevEighth	17-18	23:52:08	198.3	6.625	5000
LowElevQuarter	19-20	00:02:46	200.2	5.939	5000
MedElevEighth	21-22	00:13:42	200.3	11.18	5000
MedElevQuarter	23-24	00:24:22	202.4	10.42	5000
NGC7027	25-26	00:37:52	298.7	36.68	5000
NGC7027	27-28	00:48:30	299.6	34.86	5000
NGC7027	29-30	00:59:08	300.6	33.06	5000
NGC7027	31-32	01:09:46	301.5	31.27	5000
3C48	33-34	01:22:57	252.3	76.25	5000
NGC7027	35-36	01:36:22	304.1	26.88	5000
NGC7027	37-38	01:46:59	305.2	25.17	5000
NGC7027	39-40	01:57:36	306.3	23.47	5000
NGC7027	41-42	02:08:13	307.4	21.81	5000
NGC7027	43-44	02:18:50	308.6	20.17	5000
NGC7027	45-46	02:29:27	309.8	18.55	5000
NGC7027	47-48	02:40:04	311.0	16.97	5000
NGC7027	49-50	02:50:40	312.3	15.42	5000
NGC7027	51-52	03:01:16	313.6	13.89	5000
NGC7027	53-54	03:11:51	314.9	12.41	5000
NGC7027	55-56	03:22:26	316.2	10.96	5000
NGC7027	57-58	03:33:01	317.6	9.55	5000
NGC7027	59-60	03:43:37	319.0	8.18	5000

was 5 min and 30 sec east of the 'on' position. The flux density of NGC7027 is about 5.4 Jy at 5 GHz and 3C48 is also about 5.4 Jy. The "HighElevEighth", "HighElevQuarter", etc. are focus offset measurements at one-eighth and one-quarter wavelength subreflector offsets in the +Y direction at high (65 deg.), medium (11 deg.), and low (6 deg.) elevations.

Data display and discussion closely follows the format of the report on similar measurements at L-band of 12/26/02.

One-Eighth and One-Quarter Wavelength Subreflector Offsets

Six on-off scan pairs were recorded using 1/8- and 1/4-wavelength subreflector Y offsets at three telescope elevation angles of 6, 11, and 65 degrees. The telescope elevation was varied to change the amount of system noise coming from the atmosphere near the main beam of the antenna to try to see whether the 1.6-Mhz ripple multipath is affecting noise entering the receiving system from the forward or rearward direction of the antenna. The (on - off) / off spectra are shown in Figures 1, 2, and 3. The 'on' scans were with the subreflector displaced by 1/8 or 1/4 wavelength in the Y direction from its normal position, and the 'off' scans were taken with the subreflector at its normal focus position.

The 9-MHz ripple period is evident in all spectra, and the 1.6-MHz period

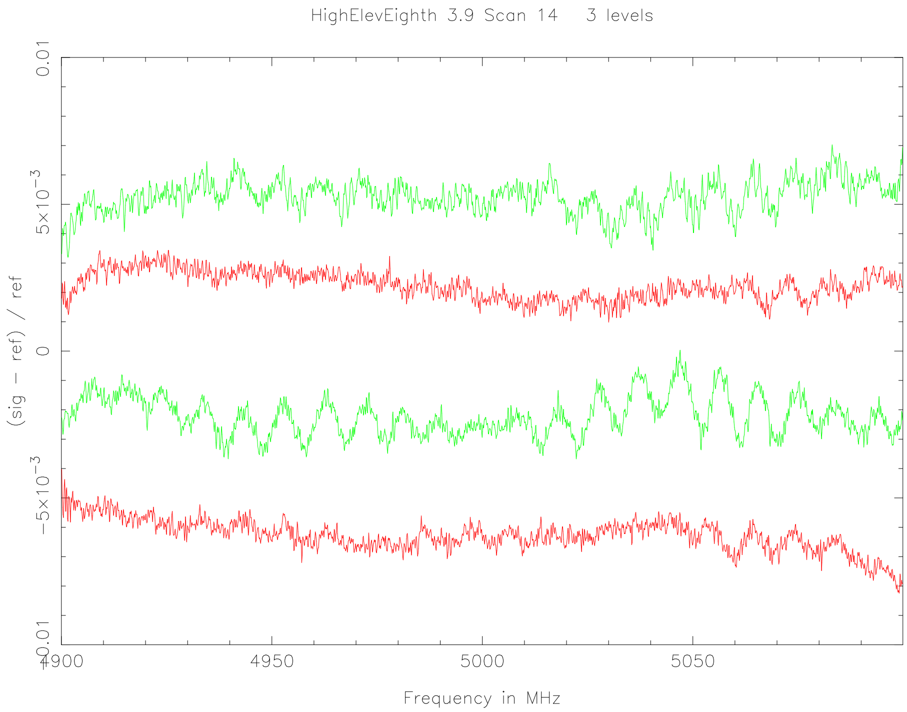

Figure 1: Scans 13-16, cold sky (on - off) / off spectra at an elevation of 80 degrees, where 'off' is with the subreflector in its nominal focus position and 'on' is with the subreflector displaced in the +Y direction. The red curves are for receiver channel X and the green curves are for channel Y. The top curves are with 1/8-wavelength (7.62 mm) displacement and the bottom curves are with 1/4-wavelength (15.2 mm) displacement. The curves are offset by a small amount in the vertical direction to separate the plots.

is seen mainly in receiver channel Y and is strongest in the 1/8-wavelength subreflector displacement spectra. To get a quantitative measure of the ripple periods and amplitudes, FFT's of all spectra shown in Figures 1, 2, and 3 are shown in Figures 4-11. The RFI spikes in the spectra were removed and a cosine taper applied to the end 10% of the spectra before doing the FFT's.

Figures 4 and 5 are FFT's of the averages of the spectra at different elevations to get the best signal-to-noise for a comparison of the two receiver channels at the two subreflector displacements. The 9-MHz ripple period corresponds to the peak around 16 meters in the FFT plots, which is the distance from the roof of the receiver room to the subreflector. This peak is strongest in the 1/4-wavelength subreflector displacement indicating that it involves only one reflection from the subreflector.

The 1.6-MHz ripple period shows up as a broad feature in the FFT curves

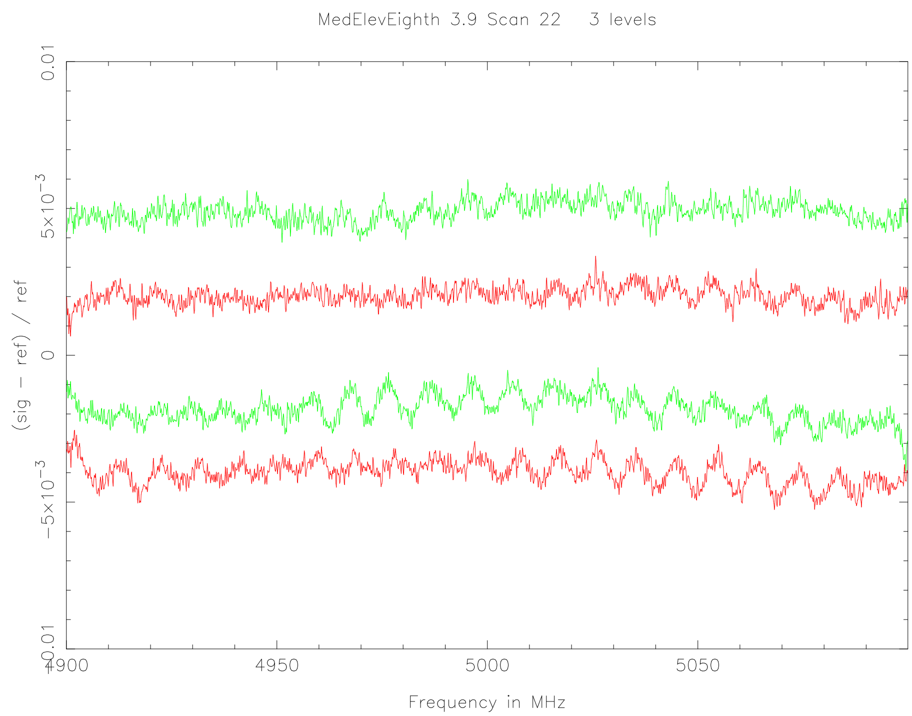

Figure 2: Scans 21-24, cold sky (on - off) / off spectra at an elevation of 11 degrees (sec(z)=5.2), where 'off' is with the subreflector in its nominal focus position and 'on' is with the subreflector displaced in the +Y direction. The red curves are for receiver channel X and the green curves are for channel Y. The top curves are with 1/8-wavelength (7.62 mm) displacement and the bottom curves are with 1/4-wavelength (15.2 mm) displacement. The bottom curves are offset by a small amount in the vertical direction to separate the plots.

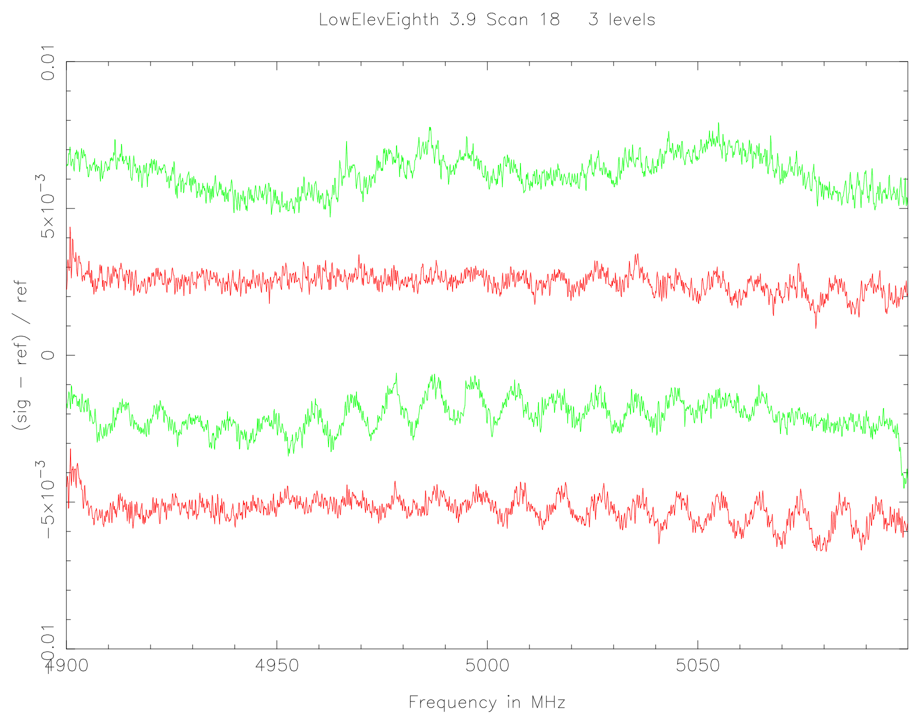

Figure 3: Scans 17-20, cold sky (on - off) / off spectra at an elevation of about 6 degrees (sec(z)=9.6), where 'off' is with the subreflector in its nominal focus position and 'on' is with the subreflector displaced in the +Y direction. The red curves are for receiver channel X and the green curves are for channel Y. The top curves are with 1/8-wavelength (7.62 mm) displacement and the bottom curves are with 1/4-wavelength (15.2 mm) displacement. The bottom curves are offset by a small amount in the vertical direction to separate the plots.

extending from about 82 to 117 meters distance in Figure 5. The range of the feed-subreflector-main reflector distances of the GBT is 80.9 to 125.9 meters so it seems very likely that this ripple involves scattering from the circumferential panel gaps in the main reflector. The amplitude of this ripple is much stronger in receiver channel Y than in X, which is to be expected since the Y polarization is perpendicular to the circumferential panel gaps and, hence, is expected to be more strongly scattered by the gaps. The fact that this ripple is strongest in the 1/8-wavelength difference spectra says that the interfering path involves two subreflector reflections as would be the case for a feed-subreflector-main reflector reflection path.

Evidently, environmental noise entering the feed is partially scattered to the subreflector. Some of this noise returns directly to the feed, causing the 9-MHz ripple. Some of this noise continues to the main reflector where it is scattered coherently by the circumferential panel gaps returning to the subreflector and the feed causing the 1.6-MHz ripple. Note that the radial panel gaps are not expected to show significant reflections to the feed because they do not run along lines of constant phase as seen from the feed as do the circumferential gaps.

A small feature in the FFT curves of channel Y can be seen at a distance of 20 meters. It may be slightly stronger in the 1/4-wavelength displacement on-off difference. The origin of this feature is unknown at the moment. Interestingly, there is little, if any, power seen in the FFT curves at a distance of 65 meters, which is the distance from the subreflector to main reflector near the main reflector axis where the two surfaces are nearly parallel. Apparently this reflection path is not a major player in the environmental noise multipath interference. There is a small feature at about 62 meters, which is probably some uncanceled 2.4-MHz ripple in the fiber optical modulators.

Figures 6-13 show the individual FFT plots at different telescope elevations for the two receiver channels and 1/4- and 1/8-wavelength subreflector displacements. In the 1/4-wavelength displacement data the 16-meter FFT feature is strongest at low elevations in the channel X spectra, but it is strongest at high elevations in channel Y. The amplitude of the 82 to 117-meter distance range of the 1/8-wavelength displacement data for channel Y is somewhat stronger at high elevations, but it's hard to make a strong case for a clear trend with elevation. This tends to argue that the major component of the noise participating in the multipaths discussed here is not entering near the main beam of the telescope. The integral of the channel Y FFT data in the 82 to 117-meter distance range of the 1/8-wavelength displacement data is given in Table 3. If anything, the integrated ripple amplitude in this distance range appears strongest a high elevation. When compared to the corresponding L-band values in Table 2 of the 12/26/02 report, the C-band ripples due to the panel gap reflections are a factor of 4 to 10 weaker relative to the total system noise power.

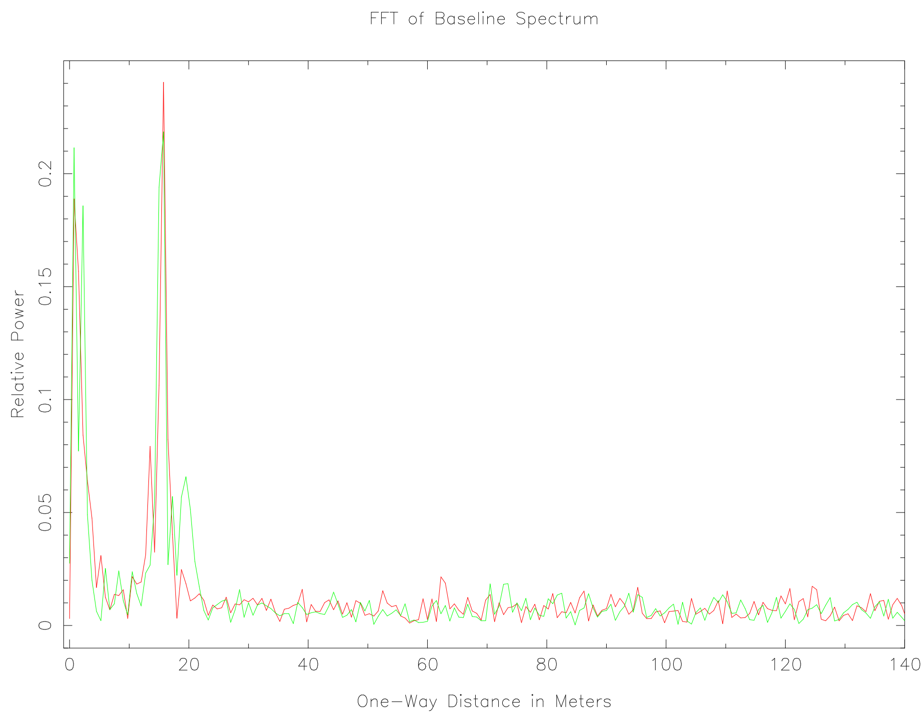

Figure 4: Scans 15, 16, 19, 20, 23, and 24; FFT's of the averages of the 1/4-wavelength displacement spectra in Figures 1, 2, and 3. The red line is receiver channel X, and the green line is channel Y. The horizontal scale is in units of one-way path-length distance from the feed in meters, assuming that the features in the FFT are due to reflections from the antenna surfaces. The vertical scale is roughly the ripple rms amplitude in units of 0.001 of the system noise power density (fraction of Tsys).

Table 3: Relative total 'off' spectrum power and FFT integral in the distance range of 82 to 117 meters in Figure 12 as a function of telescope elevation.

Elevation	sec(z)	Total Power	FFT Integ.
65	1.1	1.00	1.04
11	5.2	1.32	0.34
6	9.6	1.65	0.41

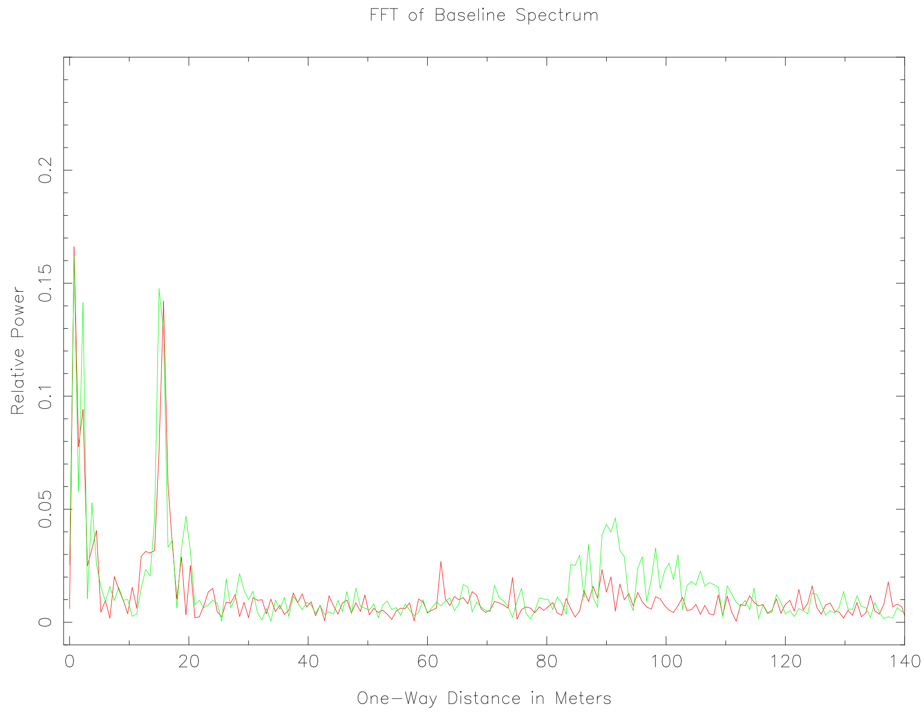

Figure 5: Scans 13, 14, 17, 18, 21, and 22; FFT's of the average of the of the 1/8-wavelength displacement spectra in Figures 1, 2, and 3. The red line is receiver channel X, and the green line is channel Y. The horizontal scale is in units of one-way path-length distance from the feed in meters, assuming that the features in the FFT are due to reflections from the antenna surfaces. The vertical scale is roughly the ripple rms amplitude in units of 0.001 of the system noise power density (fraction of Tsys).

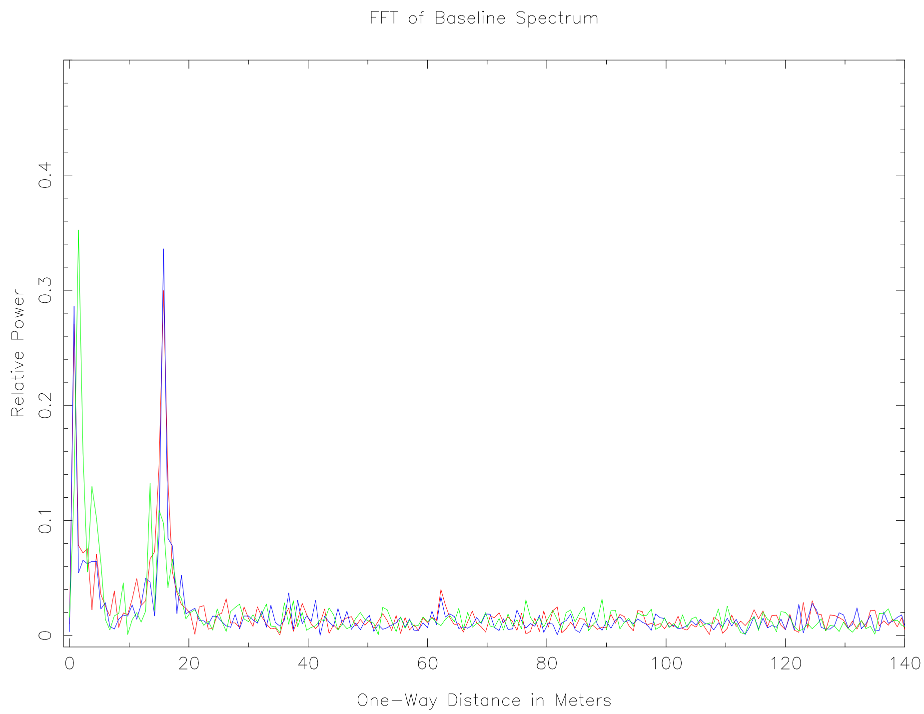

Figure 6: Scans 15, 16, 19, 20, 23, and 24; FFT's of the 1/4-wavelength displacement spectra for receiver channel X in Figures 1, 2, and 3. The red line is at 6 degrees elevation, the blue line at 11 degrees, and the green line at 65 degrees. The horizontal scale is in units of one-way path-length distance from the feed in meters, assuming that the features in the FFT are due to reflections from the antenna surfaces. The vertical scale is roughly the ripple rms amplitude in units of 0.001 of the system noise power density (fraction of Tsys). Note the vertical scale change from Figures 4 and 5.

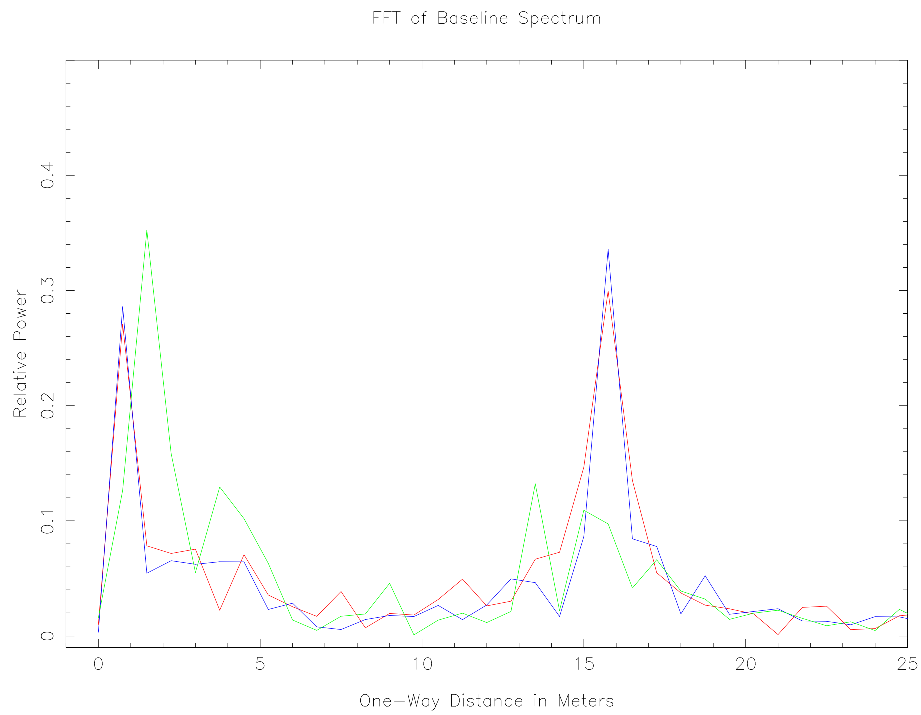

Figure 7: Scans 15, 16, 19, 20, 23, and 24; same as Figure 6 but with the horizontal scale expanded.

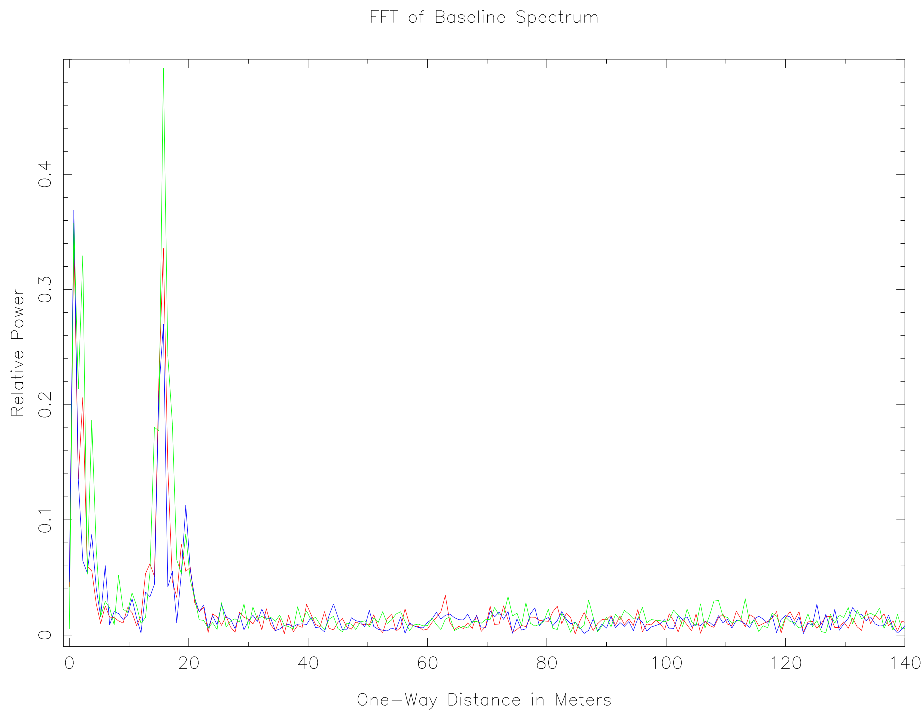

Figure 8: Scans Scans Scans 15, 16, 19, 20, 23, and 24; FFT's of the 1/4-wavelength displacement spectra for receiver channel Y in Figures 1, 2, and 3. The red line is at 6 degrees elevation, the blue line at 11 degrees, and the green line at 65 degrees. The horizontal scale is in units of one-way path-length distance from the feed in meters, assuming that the features in the FFT are due to reflections from the antenna surfaces. The vertical scale is roughly the ripple rms amplitude in units of 0.001 of the system noise power density (fraction of Tsys). Note the vertical scale change from Figures 4 and 5.

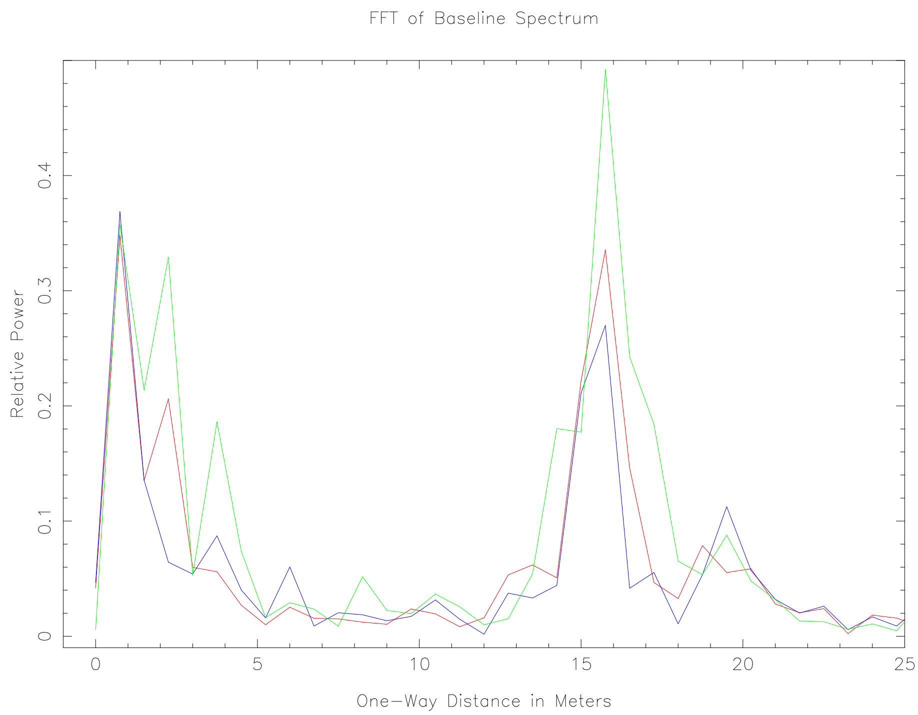

Figure 9: Scans Scans Scans 15, 16, 19, 20, 23, and 24; same as Figure 8 but with the horizontal scale expanded.

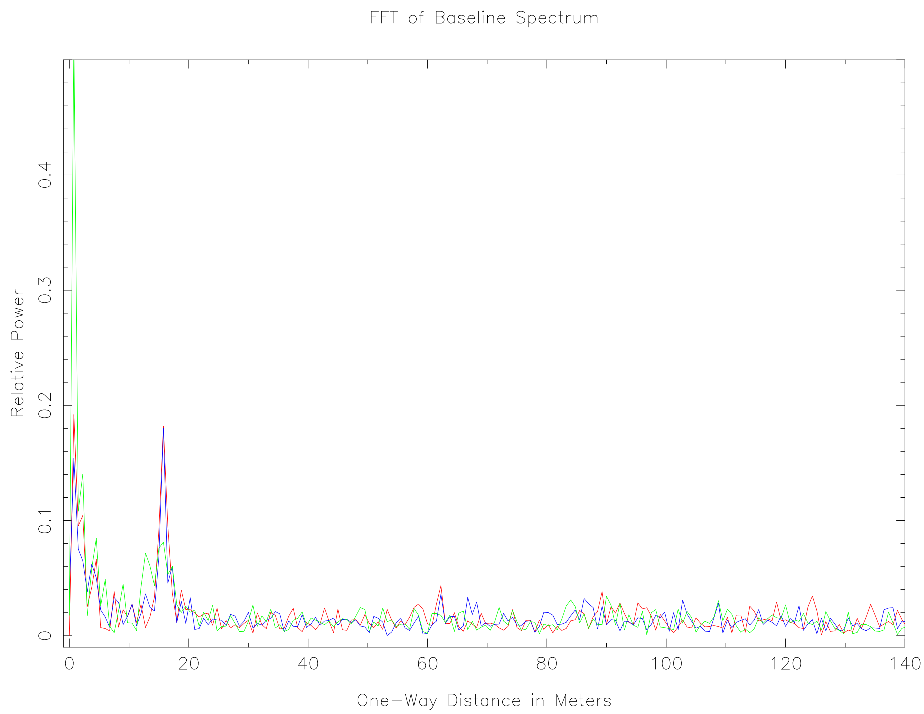

Figure 10: Scans 13, 14, 17, 18, 21, and 22; FFT's of the 1/8-wavelength displacement spectra for receiver channel X in Figures 1, 2, and 3. The red line is at 6 degrees elevation, the blue line at 11 degrees, and the green line at 65 degrees. The horizontal scale is in units of one-way path-length distance from the feed in meters, assuming that the features in the FFT are due to reflections from the antenna surfaces. The vertical scale is roughly the ripple rms amplitude in units of 0.001 of the system noise power density (fraction of Tsys). Note the vertical scale change from Figures 4 and 5.

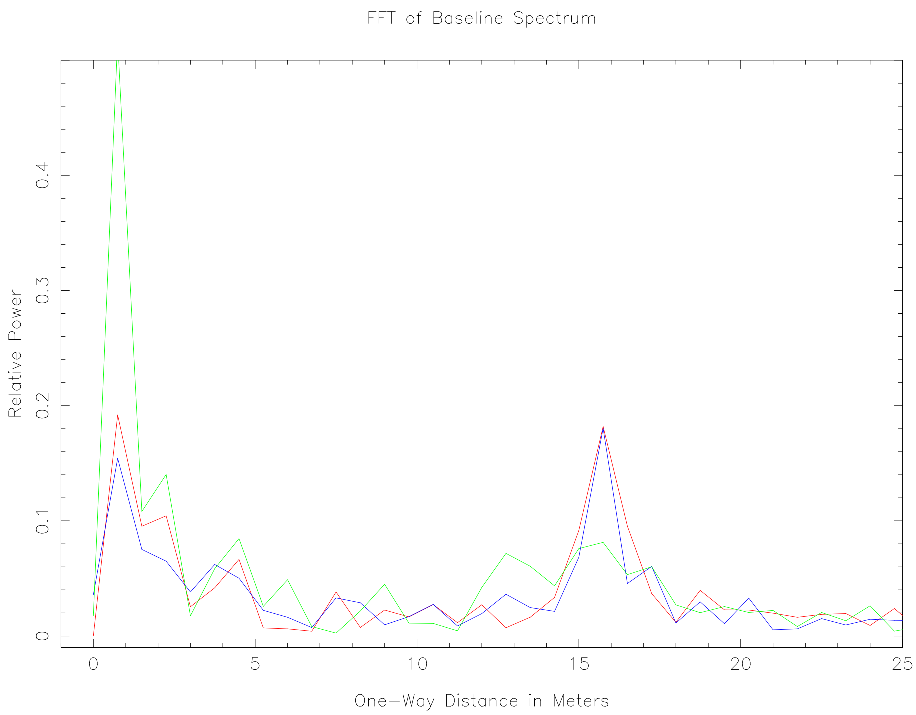

Figure 11: Scans 13, 14, 17, 18, 21, and 22; same as Figure 10 but with the horizontal scale expanded.

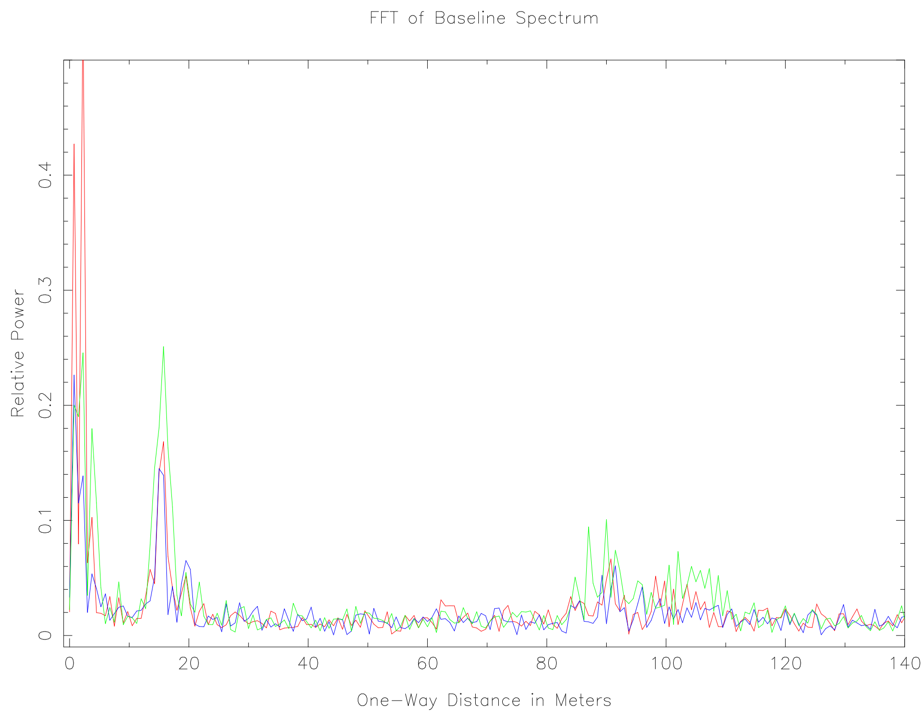

Figure 12: Scans 13, 14, 17, 18, 21, and 22; FFT's of the 1/8-wavelength displacement spectra for receiver channel Y in Figures 1, 2, and 3. The red line is at 6 degrees elevation, the blue line at 11 degrees, and the green line at 65 degrees. The horizontal scale is in units of one-way path-length distance from the feed in meters, assuming that the features in the FFT are due to reflections from the antenna surfaces. The vertical scale is roughly the ripple rms amplitude in units of 0.001 of the system noise power density (fraction of Tsys). Note the vertical scale change from Figures 4 and 5.

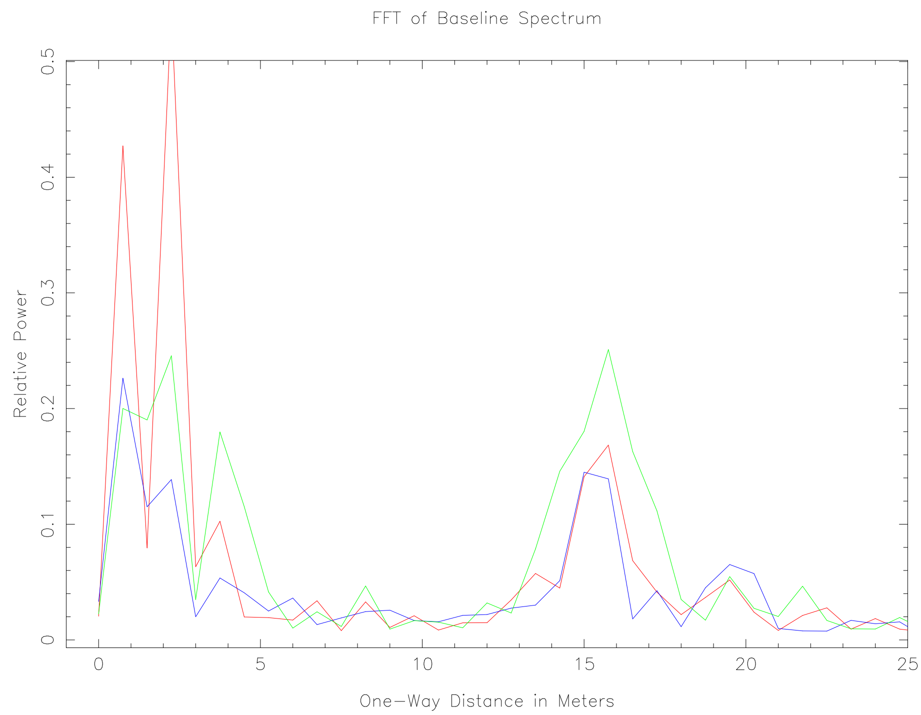

Figure 13: Scans 13, 14, 17, 18, 21, and 22; same as Figure 12 but with the horizontal scale expanded.

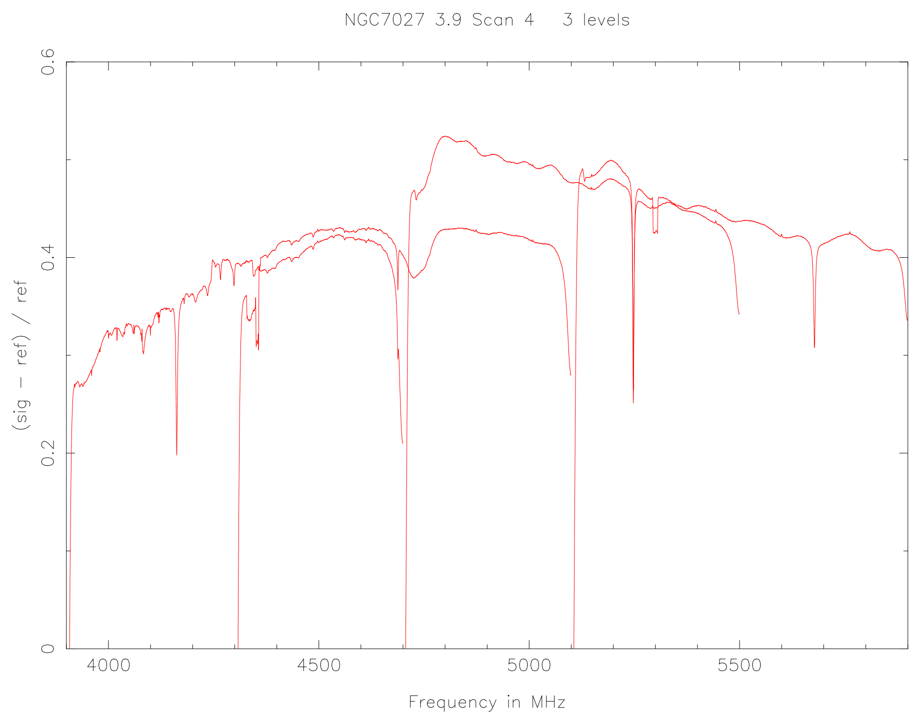

Figure 14: Scans 3, 4, and 6-11, receiver channel X (on - off) / off spectra for NGC7027 across the frequency range of the receiver using overlapping 800 MHz spectra.

Broadband Continuum Source Spectrum

Figure 14 shows the receiver channel X ratio of spectral power density from the radio source, NGC7027, to the power density from the telescope system when looking at the 'off' position on the sky, i.e., (on - off) / off. The match between overlapping spectra is not very good in either detail or average levels. There's enough match in the overlapping spectra and in the general spectrum trend to suggest that some of the structure is due to receiver components ahead of the mixer, as has been found in other receivers, but further measurements are needed to confirm this. The gain of the system appeared to be a bit unstable. Figure 15 shows the spectral ratio of 30-second records 2 through 10 to record 1 for scan 9. This scan was the least stable for receiver channel X of scans 3-11 and was the 'off' for the 4700 to 5500 MHz spectrum in Figure 14. The ripple period of about 60 MHz in Figures 14 and 15 is similar to ripples seen in IF noise spectra, which leads one to suspect an IF instability in these measurements.

The channel Y 800-MHz bandwidth spectra were plagued by a spectrometer defect so these spectra were unusable.

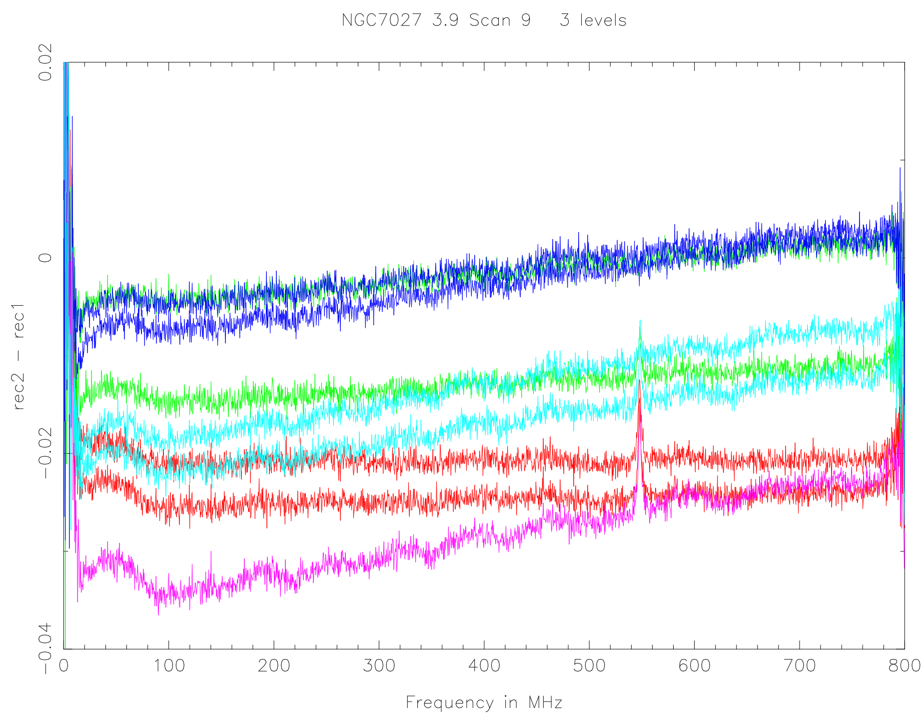

Figure 15: Scan 9, variation of spectra within one 5-minute scan. The spectra are the ratios of 30-seconds records 2 through 10 to record 1. The temporal order of the spectra are red, red, green, green, dark blue, dark blue, blue-green, blue-green, violet

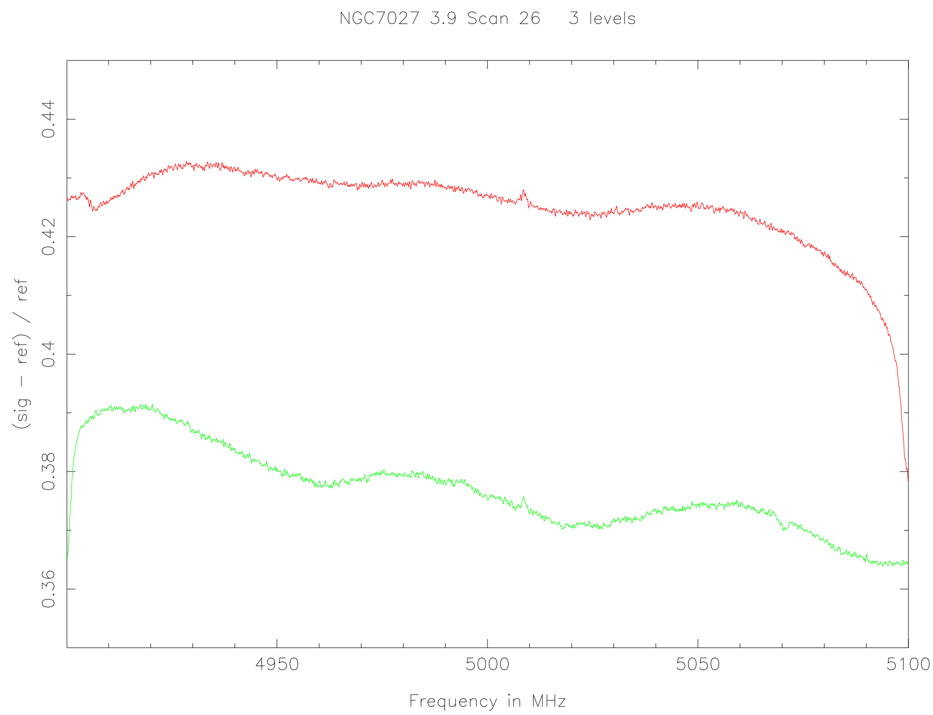

Figure 16: Scans 25 and 26; (on - off) / off spectra for NGC7027 using a 200 MHz bandwidth. The vertical scale is the fraction of system noise power density. The red curve is for receiver channel X and the green curve for channel Y.

Continuum Source Response Stability

A possible method for compensating for the frequency dependence of the telescope system response to continuum radio sources is to use a strong source with no known spectral lines to calibrate this response and apply it to continuum spectra of weaker sources in which one is searching for or measuring spectral lines. This method will depend on the stability of the telescope and receiver signal path with time and between the calibrator and measured continuum radio sources. As a first test of this stability on the C-band receiver we ran 17 on-off scan pairs on the continuum source, NGC7027 (S = 5.4 Jy), and one scan pair on 3C48 (S = 5.4 Jy). The antenna azimuths and elevations are given in Table 2.

Figure 16 shows the (on - off) / off spectra for NGC7027. The channel X spectrum is essentially a 200-MHz section of the broader spectrum shown in Figure 14. The channel Y spectrum is new since the 800-MHz mode of the spectrometer was not working correctly on the second sampler, but it was OK at 200-MHz bandwidth.

Figure 17 shows the progression with time of the (on - off) / off spectrum ratio for channel X of continuum source NGC7027. Figure 18 shows the same ratios for channel Y. These ratio spectra were remarkably stable throughout the three-hour observing period. The channel Y spectra were not as flat, but the ratio of the first two scan pairs was not significantly better that the ratio of the last and first pair. During the three hours of observing NGC7027 was moving toward the horizon so the system temperature was rising due to increasing atmospheric noise. Hence, the (on - off) / off spectrum of later scan pairs was of lower amplitude due to greater noise power in the 'off'. This effect is shown in Figure 19.

Another way to look at continuum spectra ratios is to simply take the ratios in raw spectrum values, (on - off), instead of dividing each by the off spectrum. Plots of these values are shown in Figures 20 and 21. The results are roughly the same as for the (on - off) / off spectrum ratios in Figures 17 and 18 except that the (on - off) / off spectra may be slightly flatter toward the end of the three hours. This is somewhat the opposite of results found at L-band, where the (on - off) ratios tended to be more stable when there was a difference. Except for about 3% increased atmospheric opacity, the (on - off) ratios are not expected to change with source elevation, and this what is seen in Figure 22.

To see how effectively one can calibrate the spectrum of one continuum source with another source's spectrum, we divided the spectra of 3C48 by the equivalent spectra of NGC7027. The results are shown in Figure 23. The slopes in these spectra are presumably due to a difference in the continuum spectral indices of the two sources. Aside from that, the spectrum ratio of receiver channel X is reasonably flat compared to the (on - off) / off spectrum shown in Figure 16, but the source ratio is not perfect. The results for channel Y were not as good. The (on - off) / off and (on - off) ratios were about the same, so the imperfections in the ratio spectra were probably not due to changes in the Tsys (off) spectrum between the two sources.

Figures 24 and 25 show the FFT's of the (on - off) / off and (on - off) spectra ratios, respectively, in Figure 23 after removing a constant slope from the spectra.. All four FFT's show a clear peak at a distance of 65 meters, which is the distance between the subreflector and main reflector near the axis of the main paraboloid. The amplitude of this peak is about the same in both receiver channels and both types of ratio. There is also a bit of ripple amplitude around 15 meters in the FFT plots, which may come from subreflector/feed reflections, but this feature is broad and weak so we cannot say anything conclusively. The biggest difference between the receiver channel X and Y spectra FFT's is the strong feature in channel Y at 3 meters, which corresponds to the waviness seen in Figure 23 with a period of about 35 MHz.

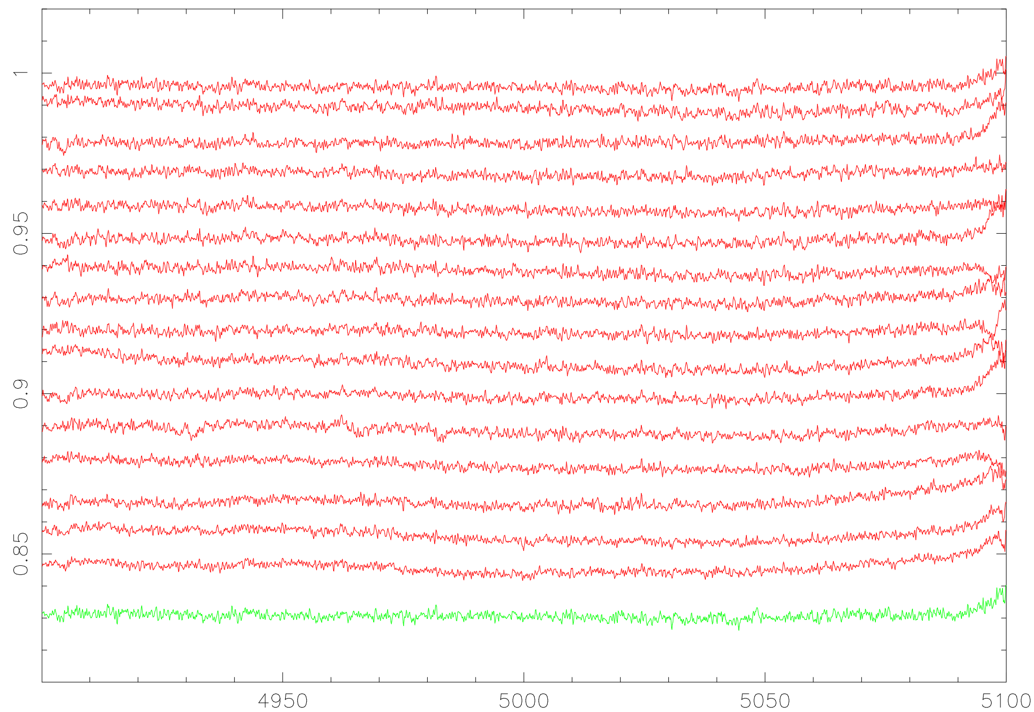

Figure 17: Scans 25-60; ratio of channel X NGC7027 continuum source (on - off) / off spectra. The top plot is the ratio of the spectrum from scan pair 27-28 to pair 25-26. The next plot down is the ratio of spectra for scan pairs 29-30 and 25-26, and so forth. The times between the scan pairs in the ratios are at intervals of about 11 minutes extending to 3 hours 5 minutes. The plots are assigned arbitrary offsets to create the time progression from top to bottom. The green plot at the bottom is a repeat of the first plot at the top for comparison of the first and last ratio spectrum.

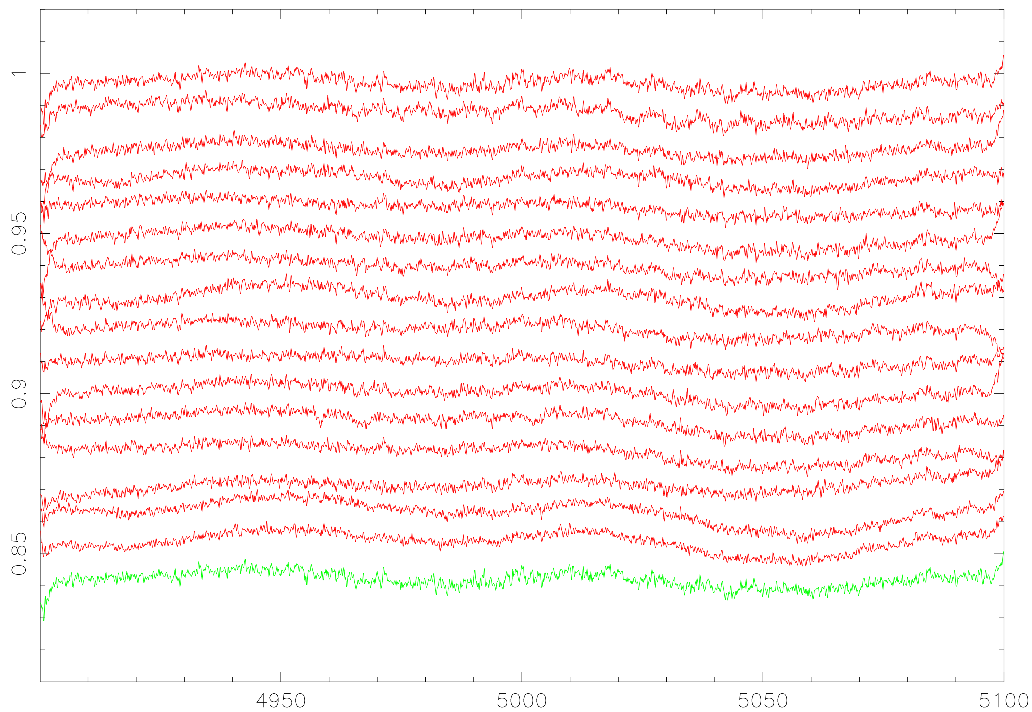

Figure 18: Scans 25-60; ratio of channel Y NGC7027 continuum source (on - off) / off spectra. The top plot is the ratio of the spectrum from scan pair 27-28 to pair 25-26. The next plot down is the ratio of spectra for scan pairs 29-30 and 25-26, and so forth. The times between the scan pairs in the ratios are at intervals of about 11 minutes extending to 3 hours 5 minutes. The plots are assigned arbitrary offsets to create the time progression from top to bottom. The green plot at the bottom is a repeat of the first plot at the top for comparison of the first and last ratio spectrum.

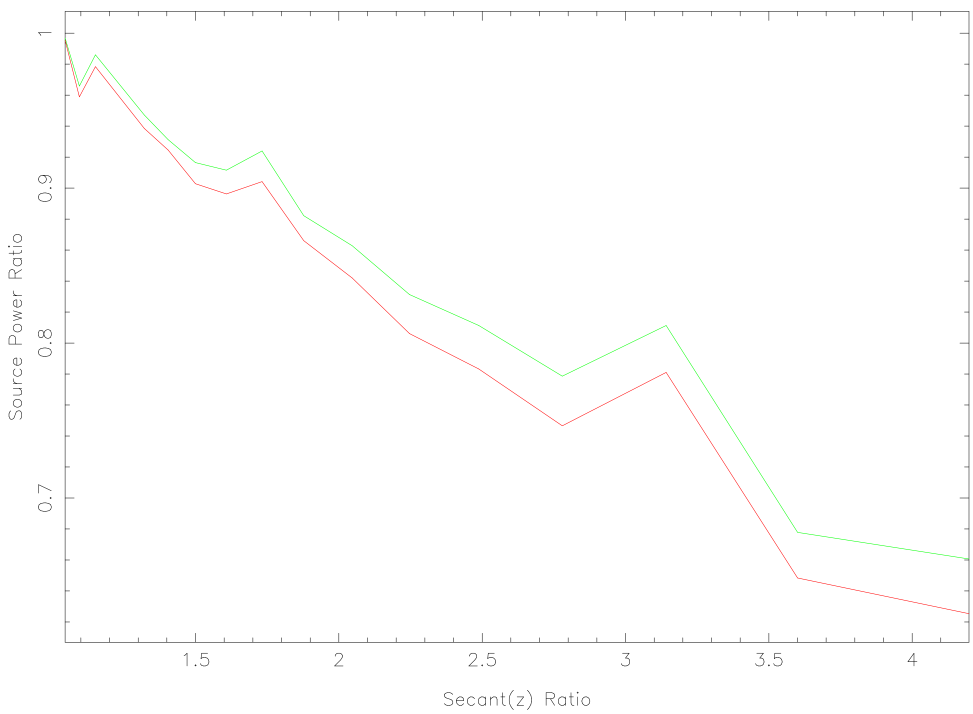

Figure 19: Scans 25-60, ratio of average power in the (on - off) / off spectra of NGC7027, shown in Figures 17 and 18, of each scan pair from 27-28 to 59-60 to the (on - off) / off average power measured in scan pair 25-26 as a function of secant(z). The red curve is for receiver channel X and the green curve for channel Y. The decreasing ratio is mostly due to increasing system temperature at lower elevations.

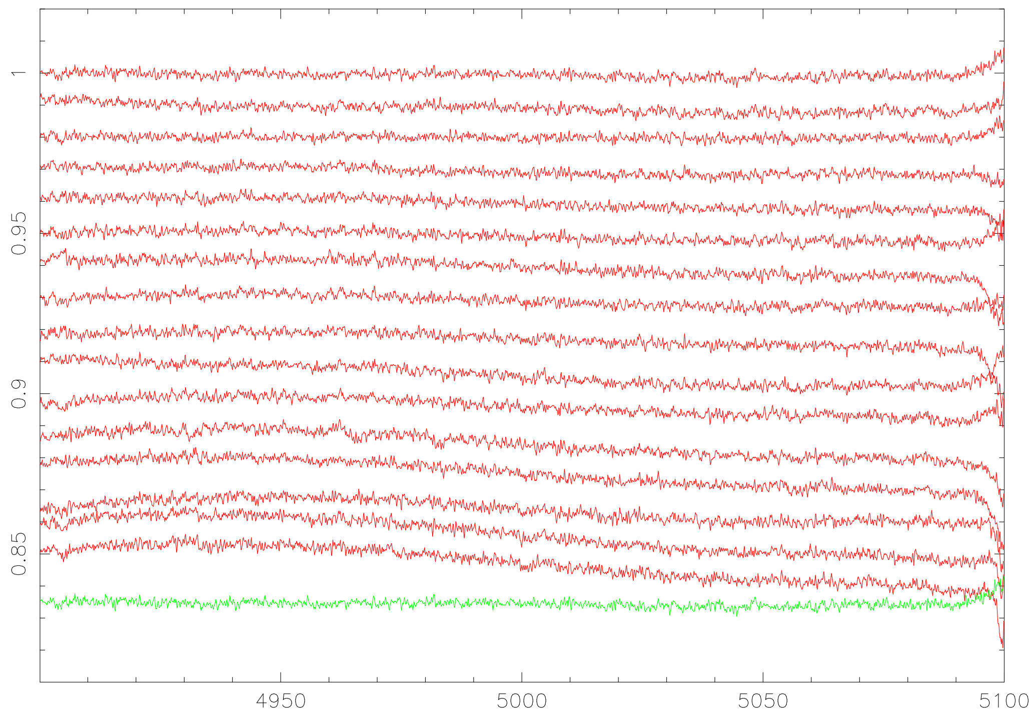

Figure 20: Scans 25-60; ratio of channel X NGC7027 continuum source (on - off) spectra. The top plot is the ratio of the spectrum from scan pair 27-28 to the spectrum from pair 25-26. The next plot down is the ratio of spectra for scan pairs 29-30 and 25-26, and so forth. The times between the scan pairs in the ratios are at intervals of about 11 minutes extending to 3 hours 5 minutes. The plots are assigned arbitrary offsets to create the time progression from top to bottom. The green plot at the bottom is a repeat of the first plot at the top for comparison of the first and last ratio spectrum.

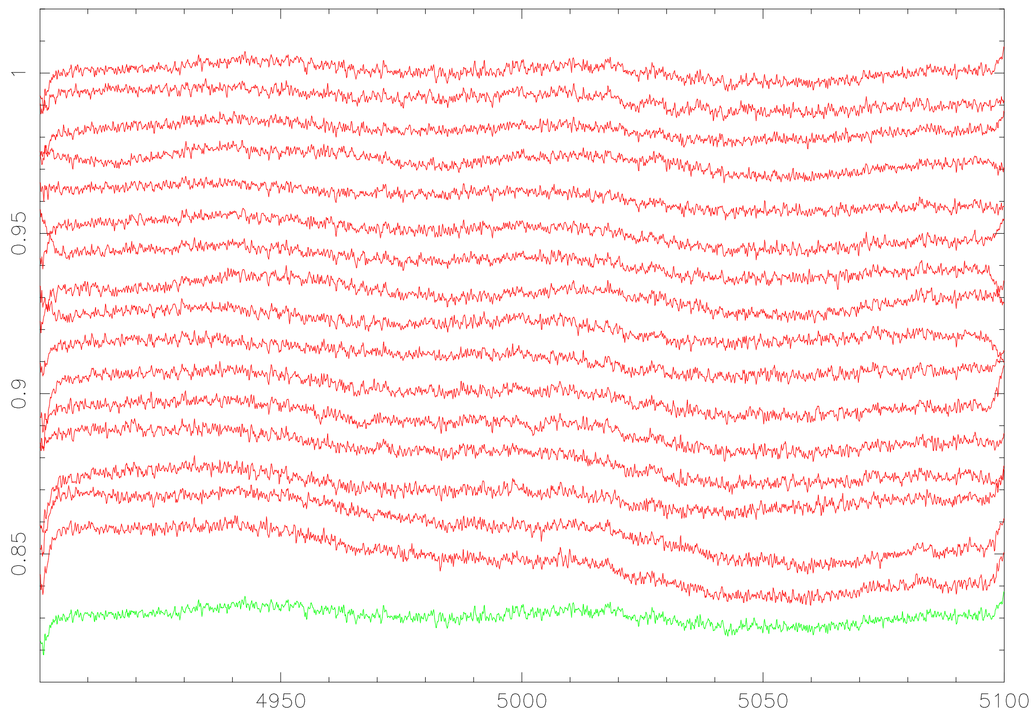

Figure 21: Scans 25-60; ratio of channel Y NGC7027 continuum source (on - off) spectra. The top plot is the ratio of the spectrum from scan pair 27-28 to the spectrum from pair 25-26. The next plot down is the ratio of spectra for scan pairs 29-30 and 25-26, and so forth. The times between the scan pairs in the ratios are at intervals of about 11 minutes extending to 3 hours 5 minutes. The plots are assigned arbitrary offsets to create the time progression from top to bottom. The green plot at the bottom is a repeat of the first plot at the top for comparison of the first and last ratio spectrum.

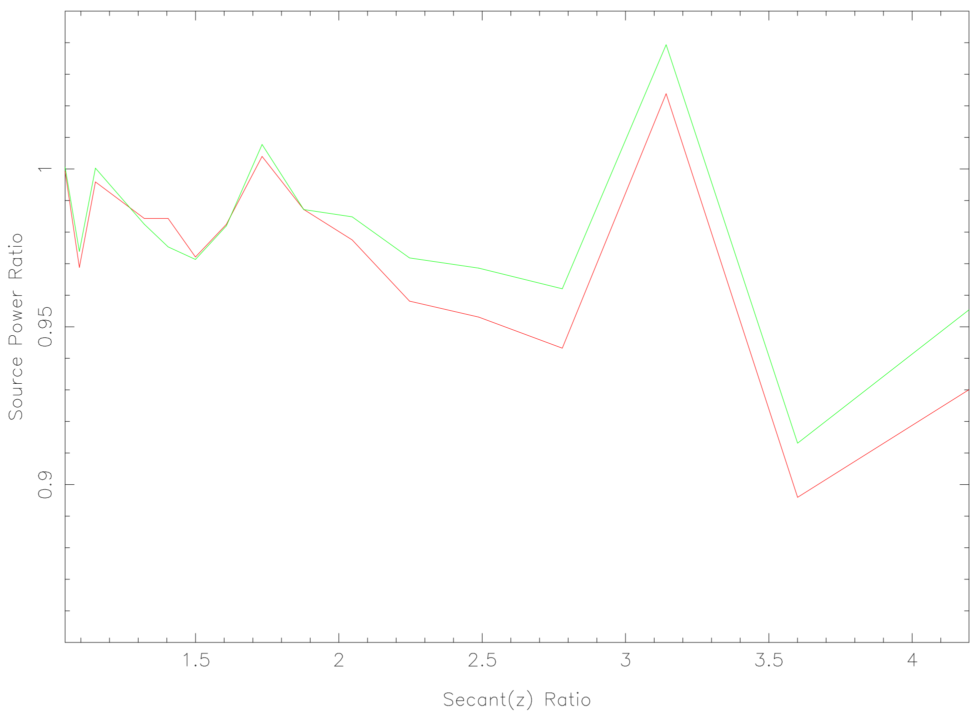

Figure 22: Scans 25-60, ratio of average power in the (on - off) spectra of NGC7027, shown in Figures 20 and 21, of each scan pair from 27-28 to 59-60 to the (on - off) average power measured in scan pair 25-26 ans a function of secant(z). The red curve is for receiver channel X and the green curve for channel Y.

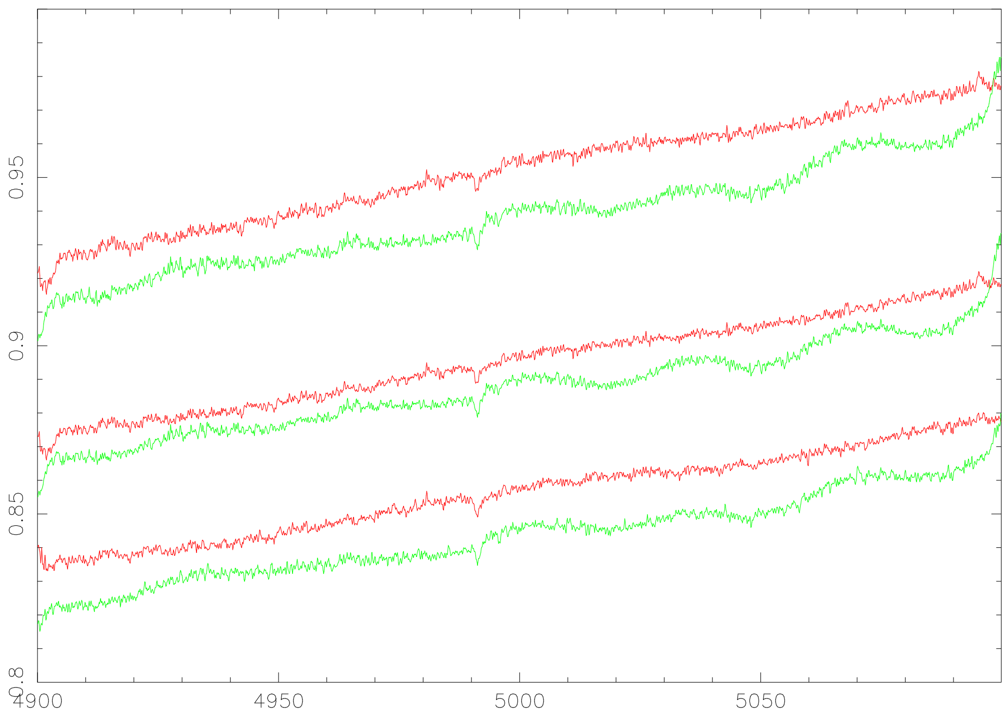

Figure 23: Scans 31-36; ratios of continuum source spectra of 3C48 to NGC7027. The top two spectra are ratio averages of (on - off) / off spectra for receiver channels X (red) and Y (green) using scan pairs 31-32 (NGC7027) and 33-34 (3C48). The middle two spectra are ratio averages of (on - off) raw spectra for same scan pairs. The bottom two spectra are ratio averages of (on - off) raw spectra using scan pairs 35-36 (NGC7027) and 33-34 (3C48). The bottom two plots are offset by about -0.05 vertically to separate the traces.

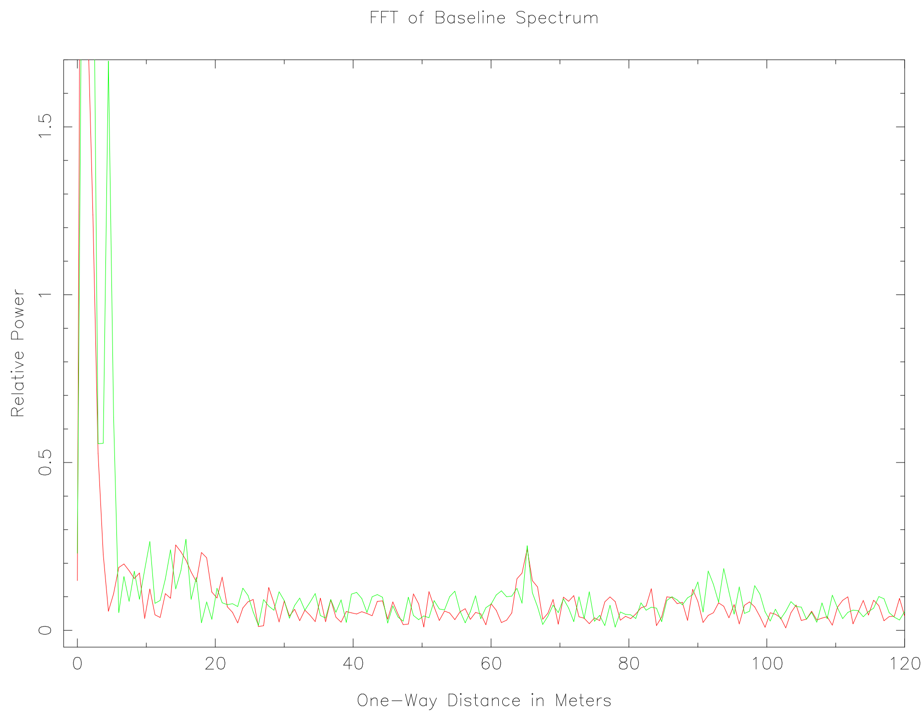

Figure 24: Scans 33-36; FFT's of the top two curves ((on - off) / off spectra ratios) in Figure 21. The horizontal scale is in units of one-way path-length distance from the feed in meters, assuming that the features in the FFT are due to reflections from the antenna surfaces. The red curve is for receiver channel X and the green curve for channel Y.

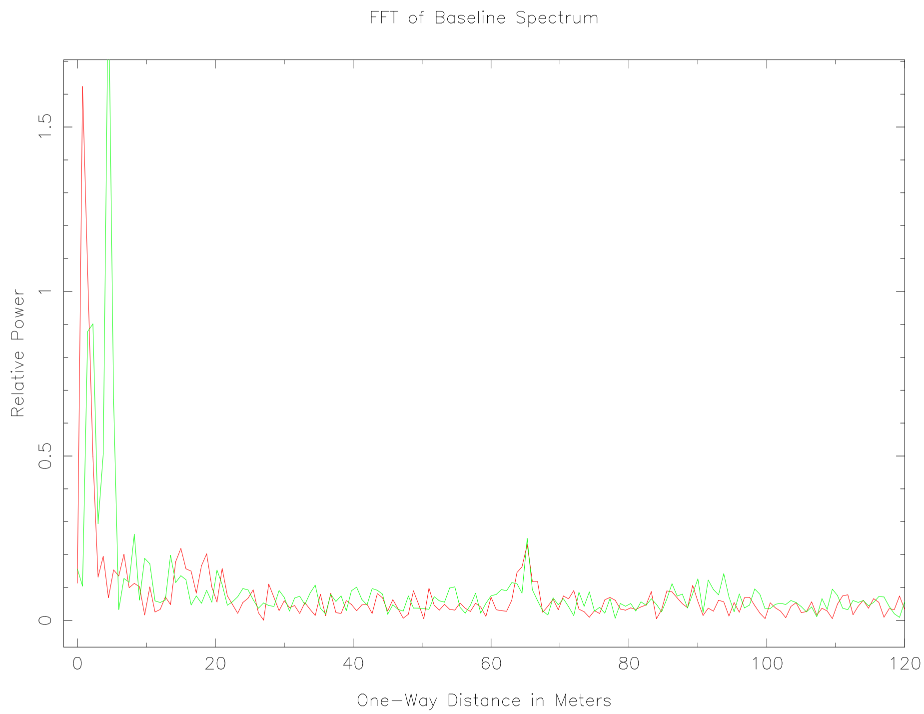

Figure 25: Scans 33-36; FFT's of the middle two curves ((on - off) spectra ratios) in Figure 21. The horizontal scale is in units of one-way path-length distance from the feed in meters, assuming that the features in the FFT are due to reflections from the antenna surfaces. The red curve is for receiver channel X and the green curve for channel Y.